Journal of Biomolecular NMR, 4 (1994) 1–16
ESCOM

J-Bio NMR 148

How is an NMR structure best defined? An analysis of molecular dynamics distance-based approaches

David A. Pearlman

Vertex Pharmaceuticals Incorporated, 40 Allston Street, Cambridge, MA 02139-4211, U.S.A.

Received 20 May 1993
Accepted 29 July 1993

Keywords: Refinement methods; Time-averaged restraints; FK506; Molecular dynamics

SUMMARY

Model studies on the macrocyclic immunosuppressive agent FK506 challenge traditional approaches to defining a structure from data collected during a 2D NMR experiment. A variety of joint molecular dynamics/NMR-distance refinement methodologies are characterized. From the results it is clear that the traditional presentation of an NMR structure as a single representative minimized conformation or as a fairly tight envelope of conformers best meeting the imposed restraints can be misleading; a greater emphasis is required on dynamics and on the fact that an NMR structure represents a time average.

INTRODUCTION

At the most rigorous level of detail, almost all chemical phenomena are extraordinarily complex. As a result, our understanding of such phenomena is generally couched in simplifications and models. This can be quite useful if the model is a good one. But it is critical that one be aware of the assumptions and failings of the model.

Sometimes a model becomes so familiar and intuitive that it blinds us to a better scientific understanding of the underlying phenomena. In many ways, the crystallographic (Blundell and Johnson, 1976) and multidimensional Nuclear Magnetic Resonance (NMR) (Wüthrich, 1986) techniques which are now used to generate the majority of structure-based molecular information have become overly reliant on such convenient-yet-misleading models. In both techniques, the result is typically presented as a single conformation, which is taken to represent the 'structure' of the molecule being studied. But, in fact, most molecules (and nearly all macromolecules) are very flexible (Petsko and Ringe, 1984; Elber and Karplus, 1987; Kessler et al., 1988; Smith, 1991), and the presentation of a single snapshot as *the* structure belies the true behavior. A detailed understanding of conformational variability is critical to generating a model which can be reliably used to interpret other experiments and as a nucleus for subsequent detailed studies. Structural chemists are certainly aware of this conformational variability, and to some extent it is reflected in the

0925-2738/$ 10.00 © 1994 ESCOM Science Publishers B.V.

B-factors determined during crystallographic refinement (Blundell and Johnson, 1976) and in the envelope of structures typically determined during NMR refinement (Clore and Gronenborn, 1989; Wagner et al., 1992). Yet in most discussions, and in most studies incorporating these structures (e.g., molecular modeling) the concept of a single 'structure' has been too appealing and comfortable to dismiss.

Here we probe the failings of this traditional description, and then determine how the structure from a multidimensional NMR experiment can better be refined and described. NMR structure determinations commonly consist of three phases (Wüthrich, 1990; James and Basus, 1991). In the first phase the data, a series of interatomic spin relaxation measurements, is collected. In the second phase, the relaxation rates are converted into interatomic distance estimates ('NOE distances'). In the third phase the distances are used to determine a 'structure'. It is this third phase that will be the focus of this paper.

BACKGROUND

Two methods are used to generate a 3D structure from a set of interatomic distances. The first is Distance Geometry (DG) (Crippen and Havel, 1988; Havel, 1991), which is very efficient at producing random structures consistent with a distance matrix. The second is molecular mechanics (minimization, Molecular Dynamics (MD), Monte Carlo, Simulated Annealing) (Burkert and Allinger, 1982; Kaptein et al., 1988; Brunger and Karplus, 1991). Molecular mechanics techniques are good at producing low-energy structures which balance the information contained in the distance set with optimization of the potential energy surface representing the molecule, but are inefficient at producing an initial guess from the distance information. Optimally, DG and molecular mechanics are used together (Liu et al., 1992). In this case, the MD phase is pivotal in refining the final 'structure'. A variety of MD simulations are run, subject to restraints based on the NMR-derived distances, and the consensus of these runs is reported as the structure. MD is an integration of Newton's equation:

$$\mathbf{F} = -dV/dx = m\mathbf{a} = m\, dx/dt^2 \tag{1}$$

giving the molecular conformation over time x(t). The integration is carried out for a specified non-zero temperature, allowing the system to sample conformational space. Here **F** is the force, V is the potential energy, x is a Cartesian coordinate, m is an atomic mass, and **a** is the acceleration. The complexity of **F** means we have to integrate this equation step-wise (in steps of 0.5–2 fs). Computer resource considerations therefore limit us to total simulations of on the order of picoseconds or nanoseconds.

In conventional MD-based NMR refinement (Nilges et al., 1988), the set of NMR-derived distances r_{NOE} is imposed on the model structure using a harmonic potential term of the form:

$$V_{NOE} = K_l(r_{model}(t) - r_l)^2 \qquad r_{model}(t) < r_l \tag{2a}$$

$$V_{NOE} = 0 \qquad r_l \le r_{model}(t) \le r_u \tag{2b}$$

$$V_{NOE} = K_u(r_{model}(t) - r_u)^2 \qquad r_u < r_{model}(t) \tag{2c}$$

$r_{model}(t)$ is the instantaneous distance in the model molecule at time t. K_l and K_u are force constants. The NMR-derived distance r_{NOE} typically lies in the middle of the range (r_l,r_u). The flat region between r_l and r_u, where the penalty function is 0 regardless of $r_{model}(t)$, accounts for experimental uncertainty in r_{NOE}. In MD/NMR refinement, these distance restraints are included as a penalty function along with the analytic function (Weiner et al., 1986), which gives the potential energy, V_{pot}, of the free molecule as a function of conformation:

$$V_{total} = V_{pot} + \Sigma V_{NOE} \tag{3}$$

Nearly all the MD-refined structures in the literature have used some variant of this approach. Sophisticated approaches which refine against the measured intensities, rather than the derived distances, have been reported (Borgias and James, 1988; Nerdal et al., 1989; Yip and Case, 1989; Baleja et al., 1990; Lane, 1990; Bonvin et al., 1991; Nilges et al., 1991; Edmondson, 1992; Mirau, 1992). However, these approaches are currently either still in the developmental stage, quite computationally intensive, and/or not yet sufficiently well characterized, so applications of these approaches have been limited.

Implicit in this formulation is the assumption that the instantaneous distances of the structure should satisfy the NMR distance restraints. In fact, the distances r_{NOE} derived from an NMR experiment represent a weighted average over the time the experiment was run (Wagner and Wüthrich, 1979), namely

$$r_{NOE} \approx \langle r(t)^{-6} \rangle^{-1/6} \tag{4}$$

This suggests that the instantaneous values of the distance $r_{model}(t)$ should be replaced by $\langle r_{model}(t)^{-6} \rangle^{-1/6}$ in Eq. 2. The resulting approach, 'time-averaged restraints', has recently been described (Torda et al., 1989) and tested (Torda et al., 1990; Pearlman and Kollman, 1991). A model study comparison of standard and time-averaged refinement methods for a DNA system (Pearlman and Kollman, 1991) indicated the time-averaged method was superior in defining the fine structure and inherent flexibility of the molecule. Note that the reciprocal weighting reflected in r_{NOE} means that r_{NOE} can be substantially smaller than $\langle r(t) \rangle$, adding to the potential errors in the standard refinement approach.

To apply refinement techniques to a real (experimentally determined) data set would not be particularly enlightening for our purposes; we would like to assess how true the results of various refinement methods and interpretations are to the actual conformational behavior of the molecule being studied, and for a real data set we cannot know this actual behavior. So, instead, we use an unrestrained MD calculation to determine the averaged distances between atom pairs for which distances could be assigned in an NMR study. These comprise our set of simulated 'experimental' distances. An additional advantage of using a simulated set of 'experimental' distances is that the force field we use in the MD refinement stages is then effectively exact. That is, in the absence of restraints, the force field will exactly reproduce the 'experimental' structure. These studies focus on the conformationally restrained macrocyclic immunosuppressive molecule FK506 (Schreiber, 1991; Van Duyne et al., 1991), and the interproton distances comprising the restraint set are those for which NOE distances were assigned in a recent NMR determination of the solution conformation of FKBP-12-bound FK506 (Lepre et al., 1992).

METHODS

All MD simulations were carried out on the immunosuppressive FK506 macrocycle, using the Amber/Sander refinement program (Pearlman et al., 1991). Nonbonded and standard internal parameters for the potential function representing FK506 were taken from the force field by Weiner et al. (1986). An all-atom model was used. Torsional parameters for special functional groups not in the standard force field were taken from Pranata and Jorgensen (1991). Partial charges were generated using an MNDO calculation (Clark, 1985) on the entire molecule. Simulations were run in vacuo; a distance dependent dielectric constant was used to mimic solvent effects. All nonbonded interactions were included. Simulations were run at constant temperature (300 K).

Standard restraints were imposed using Eq. 2. In the time-averaged restraint simulations, $r_{model}(t')$ was replaced by

$$< r_{model}(t') > = < r_{model}(t')^{-3} >^{-1/3} \approx (\int_0^{t'} e^{(t-t')/\tau} r_{model}(t)^{-3}\, dt \,/\, \int_0^{t'} e^{(t-t')/\tau}\, dt)^{-1/3} \quad (5)$$

The exponential damping factor is used to ensure that in long simulations the most recent observations $r_{model}(t)$ have a nonnegligible influence on the dynamics. For all simulations described herein, $\tau = 20$ ps. An examination of refinement results vs. τ indicated that a value of $\tau \geq 10$ ps was optimal for these simulations (D.A. Pearlman, unpublished results). An inverse weighting factor of r^{-3} (rather than r^{-6}) was chosen to typify the value one would use in most refinement protocols for experimentally derived data. It has been argued (Kessler et al., 1988) that r^{-3} weighting is more appropriate for refinements where the MD simulation length is short compared to the rotational correlation time, τ_c. In fact, for a small macrocycle such as FK506, τ_c may be on the order of half a nanosecond (e.g., the value seen for cyclosporin (Dellwo and Wand, 1989)). Thus r^{-6} refinement might be more suitable if we were refining experimentally derived data for this molecule with nanosecond-length simulations. Since, for the work reported here, the same inverse weighting factor was used in deriving the target distances and during refinement, the reciprocal weighting factor should not materially change the conclusions.

The required forces dV_{NOE}/dx were calculated using a 'pseudo-force' formulation. In the pseudo-force formulation, the exact chain rule expression for the forces,

$$\begin{aligned} F_{NOE,x}(t) &= -\partial V_{NOE}/dx \\ &= -(\partial V_{NOE} / \partial < r_{model}(t) >)(\partial < r_{model}(t) > / \partial r_{model}(t))(\partial r_{model}(t)/\partial x) \end{aligned} \quad (6)$$

is replaced by the alternate expression

$$F_{NOE,x}(t) = -(\partial V_{NOE} / \partial < r_{model}(t) >)(\partial r_{model}(t) / \partial x) \quad (7)$$

Both formulations serve to force the restraints towards the flat region of the harmonic well, but the pseudo-force formulation avoids instabilities in the MD trajectory and does not automatically diminish the magnitude of the effective force constant as the number of points used to calculate the average increases (Torda et al., 1990; Pearlman and Kollman, 1991).

Each MD simulation started with the minimized FKBP-12-bound solution conformation of

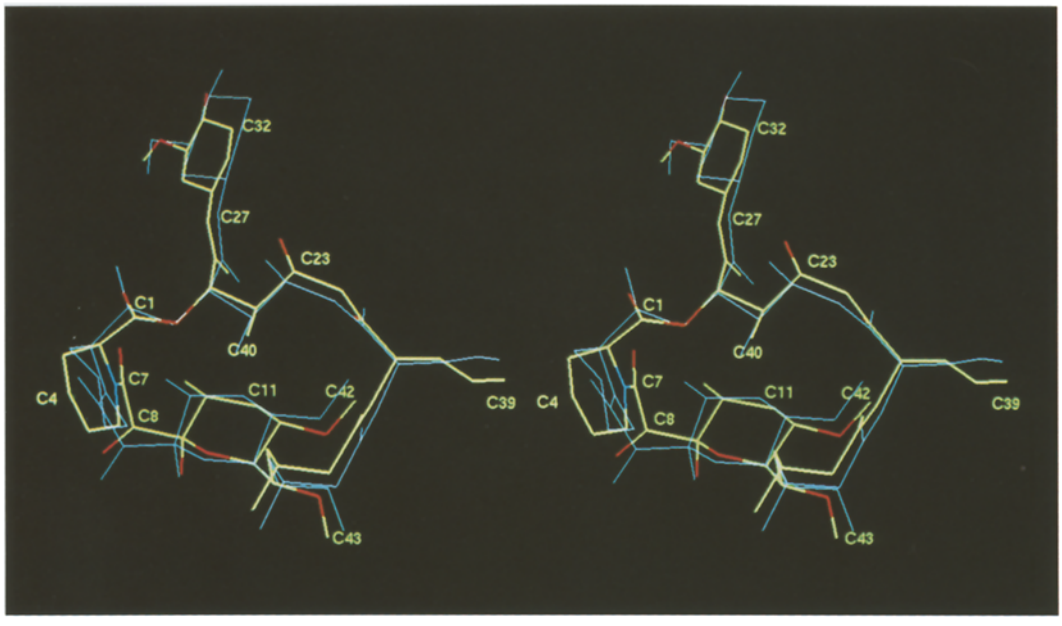

Fig. 1. Stereo representation of the averaged conformation for the 3-ns unrestrained MD simulation of FK506. Carbon atoms are in green, oxygen atoms are in red, and the nitrogen is in blue. Hydrogen atoms are not shown. For comparison, the least-squares best-fit heavy atom superposition of the experimentally determined solution structure of FK506 bound to FKBP-12 (Lepre et al., 1992) is shown in thin light blue lines (RMSD = 0.66 Å for all heavy atoms). Numbering follows the convention of Lepre et al. (1992), and a number of atoms around the macrocycle are labeled for ease of comparison with the results in that paper.

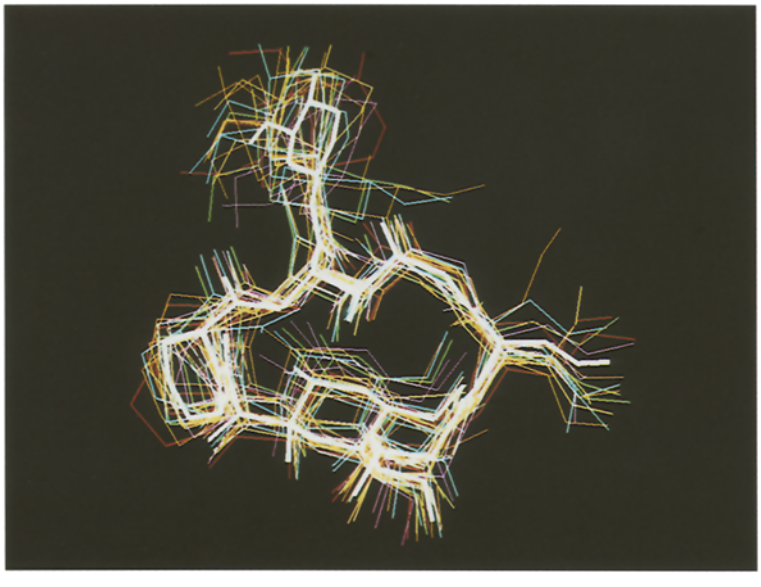

Fig. 2. A representative envelope of conformations sampled along the 3-ns unrestrained MD simulation of FK506. An RMS best-fit superposition (using all heavy atoms) of snapshots every 150 ps along the trajectory is shown. Hydrogen atoms are not shown. The averaged conformation for the entire 3-ns simulation is shown in heavy white lines.

FK506. In this conformation, the C2-N1-C7-C8 amide torsion is trans. For free FK506 in solution, a second conformation where the C2-N1-C7-C8 torsion is cis has also been observed experimentally (Karuso et al., 1990; Mierke et al., 1991). However, we have performed a torsional driving minimization study for this torsion that indicates the barrier to interconversion between the conformers is about 15 kcal/mol for unbound FK506, in vacuo. Hence, expectedly, no interconversion was observed in any of our 300 K simulations. This torsion was similarly invariant in an earlier 300 K MD simulation of FK506 in explicit solvent (Pranata and Jorgensen, 1991). Interconversion could be effected by an MD simulation at an elevated temperature (Lepre et al., 1992).

To generate an 'experimental' set of NOE distances, an unrestrained 3.2 ns MD simulation was performed. The r^{-3} weighted average value of each proton–proton distance for which an NOE distance was assigned in a recent NMR examination of FKBP-12-bound FK506 (66 distances) (Lepre et al., 1992) was determined over the final 3.0 ns. These distances were used as restraints in all subsequent refinement simulations. For restraints to methyl-group protons, the center-of-mass position of the three methyl protons was used. Six broad (120° flat well) torsional potentials were also included on the pipecolinyl ring (N1–C6) for consistency with the previous experimental refinement. Each refinement was carried out for 1 ns, storing the conformation every 1 ps for subsequent analysis. The first 200 ps of data for each refinement were discarded to minimize equilibration and thermalization effects.

Throughout this paper, we refer to 'averaged' structures. Each averaged structure was generated by first determining the root-mean-squared (RMS) best-fit superposition of each stored coordinate snapshot with the first coordinate set included in the average. Then the simple coordinate average of all these superimposed coordinate sets was taken. No minimization or regularization was carried out on any structure presented or discussed in the paper.

RESULTS

FK506 presents an excellent model system for testing refinement methodology. While it exhibits conformational flexibility, particularly at some of the pendant groups, the macrocycle imparts considerable order, making reasonably thorough sampling possible with MD techniques. Figure 1 shows the average structure of FK506 from the 3-ns unrestrained MD simulation. The average structure is surprisingly similar (RMSD = 0.66 Å) to the recently published solution structure of FKBP-12-bound FK506 (Lepre et al., 1992), shown in thin, light blue lines. The reader is referred to that paper for detailed conformational analysis. To ensure this conformation reasonably reflects a converged average, a second 3.2-ns simulation was run with a different set of starting velocities (and hence different trajectory). The RMSD between the averaged structure from this run and that of the first was only 0.07 Å (macrocycle) and 0.20 Å (all heavy atoms), implying 3 ns of sampling is sufficient to achieve convergence.

In Fig. 2, a series of 30 snapshots, corresponding to every 150 ps, is plotted for the unrestrained FK506 MD simulation. This envelope represents the source of the 'experimental' restraints, and ideally we would like to reproduce the information imparted by this picture with the restrained MD simulations. The structure shown in heavy white lines is the average over the entire 3 ns simulation. Note that the structure is particularly flexible in the cyclohexyl (C28–C33) and allyl (C37–C39) regions. The conformational variability of the structure can be quantified in a plot of

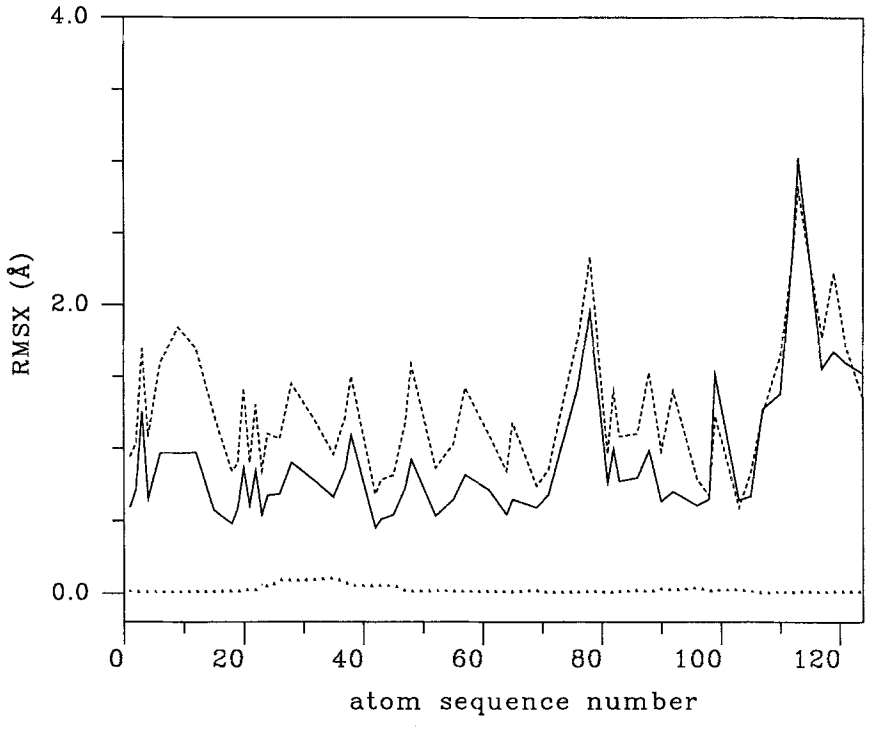

Fig. 3. The RMS fluctuations about mean positions (RMSX) of the heavy atoms of FK506 for the unrestrained 3-ns trajectory of Fig. 2 (solid line). Also shown are the RMSX plots corresponding to standard restraints, double-sided wells, $P_u = P_l = 0.75\sigma$, and $K_u = K_l = 36$ kcal/mol (dotted line), and to time-averaged restraints, double-sided wells, $P_u = P_l = 0.75\sigma$ and $K_u = K_l = 36$ kcal/mol (dashed line). σ is the standard deviation in the average value of the distance in the unrestrained simulations. Atoms 4–18 correspond to the pipecolinyl ring; atoms 23–43 correspond to the pyranose ring; atoms 73–78 correspond to the allyl region; and atoms 105–124 correspond to the cyclohexyl group.

the RMS fluctuation of each heavy atom about its mean position versus atom number, the solid line in Fig. 3. From this data, it is clear that the traditional description of molecular structure in terms of a single static conformation is inappropriate.

To test the ability of standard refinement methods to reproduce the true experimental picture, two different series of simulations were carried out. In the first series, the distance restraints were imposed as upper bounds only (with the lower bound determined by van der Waals repulsion, i.e., $r_l = 0$). In the second series, double-sided harmonic wells were used. Both series consisted of 11 simulations (i = 0,10). For each restraint, $P_u = i*0.25*\sigma$, where σ is the standard deviation in the average value of the distance being restrained in the unrestrained simulation. In the double-sided wells series, $P_l = P_u$. P_l and P_u are flat-well 'Play' indices: $P_u = r_u - r_{NOE}$ and $P_l = r_{NOE} - r_l$ (see Eq. 2). Force constants $K_l = K_u = 36.0$ kcal/mol were used in every case. The averaged structures for each member of both of these series of simulations are compared to the unrestrained average in Figs. 4a and 5a. The simulations using single-sided bounds (Fig. 4a) produce a set of average structures in reasonable accord with the 'true' average. Note the small but nonnegligible amount of systematic deviation of the average with P_u. By comparison, the simulations with double-sided restraints produce a set of average conformations which reproduce the true average considerably

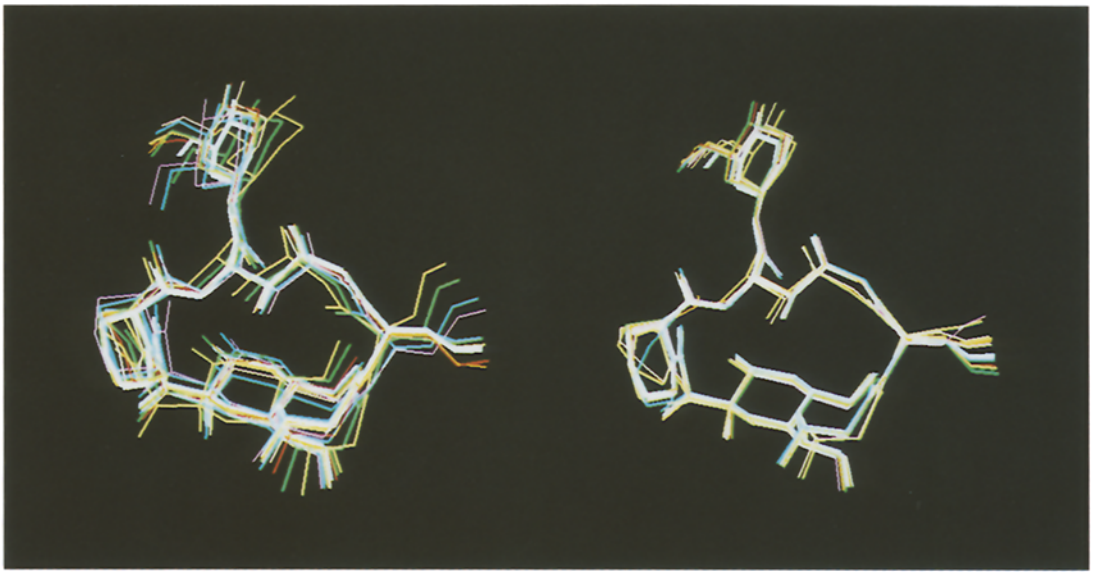

Fig. 4. The averaged conformations for the series of refinements using single-sided (upper bound only) restraints. Each series corresponds to flat-well widths $P_u = i*0.25*\sigma$, i = [1,10], where σ is the standard deviation in the average value of the distance in the unrestrained simulations. Target distances r_{NOE} were derived from the 3-ns unrestrained simulation. $K_u = K_l = 36$ kcal/mol. All averages were calculated from the final 800 ps of a 1-ns simulation. The 'true' averaged conformation for the 3-ns unrestrained simulation is shown in heavy white lines. Hydrogen atoms are not shown. Each restrained average structure has been best-fit to the unrestrained average. Figure 4a (left): Standard refinement; Fig. 4b (right): Time-averaged refinement.

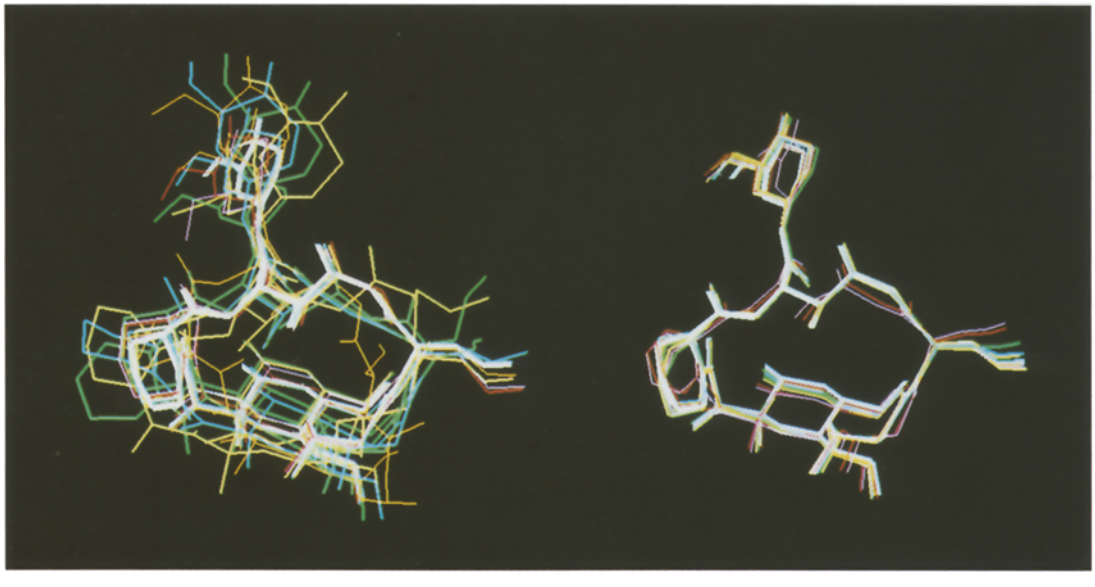

Fig. 5. The averaged conformations for the series of refinements using double-sided (upper and lower bounds) restraints. $P_l = P_u = i*0.25*\sigma$, i = [1,10]. The figure is otherwise completely analogous to Fig. 4. Figure 5a (left): Standard refinement; Fig. 5b (right): Time-averaged refinement.

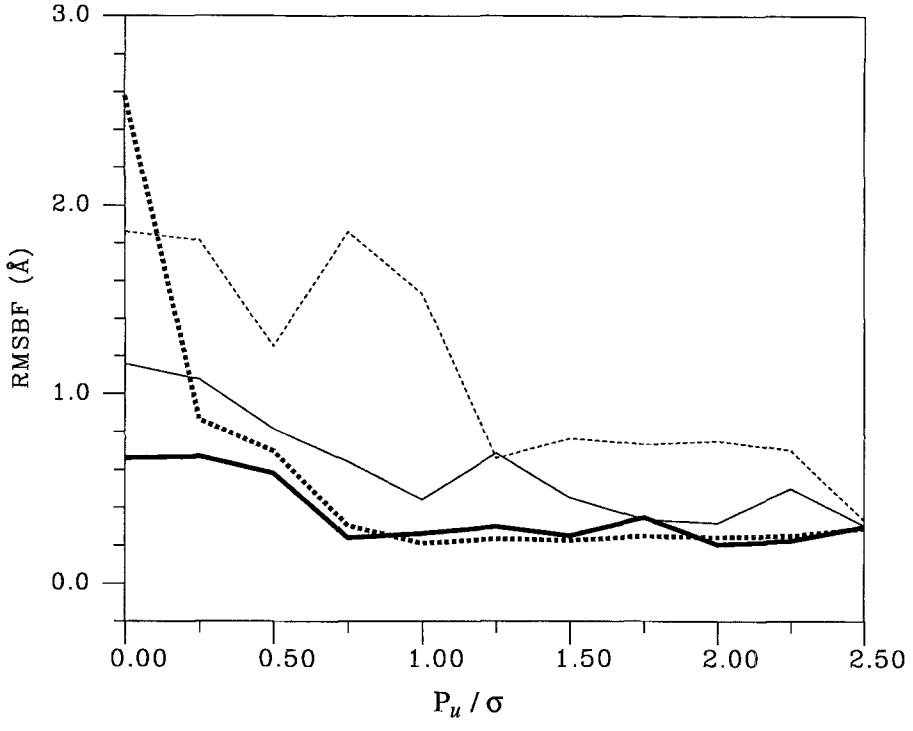

Fig. 6. RMS coordinate differences after least-squares best-fit superposition (RMSBF) between the averaged refined structures and the average structure from the 3-ns unrestrained simulation. RMSBF values are for all heavy atoms. RMSBF is plotted against P_u/σ (= P_l/σ) for standard, single-sided wells (thin solid line), standard, double-sided wells (thin dashed line), time-averaged, single-sided wells (thick solid line), and time-averaged, double-sided wells (thick dashed line). $K_u = K_l = 36$ kcal/mol in each case.

more poorly (Fig. 5a). This reflects the error introduced by the inability of any single snapshot in traditional refinement to instantaneously satisfy all of the experimentally derived time-averaged target values. Double-sided wells exacerbate the problem by introducing greater conformational restriction. One might therefore be tempted to conclude that only single-sided restraints should be used with standard refinement. But the downside of this approach is that such restraints impart much less information, and may not yield an acceptable amount of detail. This is best understood by extrapolation to the case where the upper bounds on the restraints are also removed, i.e., to the case where there are no restraints. Then the averaged structures will perfectly reflect the force field, but none of the experimental data. In real refinement, the force field is never perfect, and we wish to introduce as much experimental detail (via restraints) as possible.

By comparison, the averaged structures for simulations incorporating time-averaged restraints are in strikingly better agreement with the 'true' average. The same two series of simulations (both single- and double-sided restraints) described above for standard restraints were run with time-averaged restraints. The resulting averaged structures are compared to the unrestrained average in Figs. 4b and 5b. Note how tightly converged the averaged structures are about the true average. Figure 6 quantifies the differing qualities of the averaged structures from standard and time- averaged restraints. It is clear that time-averaged restraints can better reproduce the true

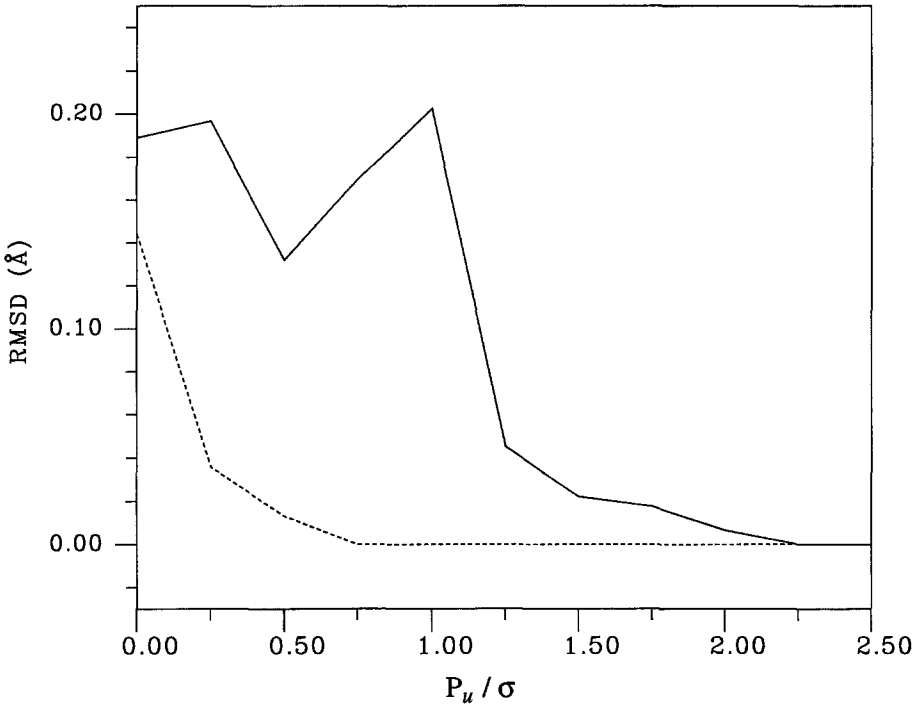

Fig. 7. RMSD, the RMS difference between the target distance values and the actual model distance values (final values for standard refinement, or average values for time-averaged refinement), as a function of P_u/σ (= P_l/σ). Solid line: Standard refinement, double-sided wells. Dashed line: Time-averaged refinement, double-sided wells.

average, regardless of the width of the flat region. This is important, since in a real NMR experiment the width of the flat region is only an estimate of the error and for different restraints will likely correspond to different multiples of the true RMS fluctuation. (Note that in Fig. 6, both standard and time-averaged refinement methods converge to a value of RMSXX of about 0.40 for large values of P_u. The non-zero residual reflects the fact that after 800 ps, a small residual sampling error remains in determining the converged average conformations of the macrocyclic substituents.)

It is critical that one not misinterpret Figs. 4 and 5. Stylistically, these figures (and Fig. 9) resemble the ensembles often presented in NMR refinement papers to represent a series of final minimized (or DG) structures which reasonably satisfy the applied restraints. But the ensembles in Figs. 4 and 5 are different. Each structure represented is an unminimized *averaged* structure corresponding to an entire restrained simulation. The envelopes of structures are *not* snapshots along a trajectory, and they do *not* represent the diversity of conformations in accord with a specific set of refinement restraints. Instead, the diversity of conformations reflects how changes in the refinement protocol (here, the width of the 'flat region') change the averaged structures sampled over entire 0.8-ns trajectories. This explains why, for example, the envelope of standard refinement conformations is tighter in Fig. 4 (where single-sided restraints are used) than in Fig. 5 (where double-sided restraints are imposed). Single-sided restraints allow greater conformational variability during any single simulation. But exactly because of this, the *averaged* structures for

all such simulations are more like one another. Two-sided restraints impose greater restrictions on each trajectory, and so the *averaged* structures more strongly reflect the varying refinement conditions (well width). Similarly, the relatively narrow widths of the conformational envelopes corresponding to time-averaged refinement (the righthand sides of Figs. 4 and 5) imply that the *averaged* structures from these refinements are relatively insensitive to either the width of the flat well, or to whether single- or double-sided wells are used. They do *not* imply that time-averaged simulations are more conformationally restrained (sample less conformational space). In fact, the opposite is true, as will be seen shortly.

RMSD, the RMS fit of the distance restraint target values to the distances in the resultant model structures, has frequently been used as an indicator of whether the general neighborhood of the correct average structure has been determined, and of whether there are any bad NMR distance assignments. In a case such as the present, where we know we are near the correct average and the distance assignments are 'exact', the residual RMSD can also be used to differentiate the appropriateness of the refinement protocol. Figure 7 presents RMSD versus P_u (= P_l) for the full-harmonic restraint refinement. There it can be seen that time-averaged restraints allow vanishingly small restraint violations in cases were $P_u \neq 0$, while for standard restraints a residual violation remains until P_u is fairly large. This reflects the difference between $r_{model}(t)$ and $r_{NOE} \propto < r(t)^{-3} >^{-1/3}$.

As important as being able to derive the appropriate average structure is the ability to impart a correct sense of the intrinsic variability of the structure. We saw (Fig. 2) that while the FK506 molecule has a well-defined average conformation, it also undergoes substantial conformational variability about this average. In this regard, the differences between using standard and time-averaged restraints are even more pronounced. Figure 8 displays snapshots along single trajectories using double-sided wells, $P_u = P_l = 0.5\sigma$, and $K_l = K_u = 36.0$ kcal/mol. The standard refinement trajectory (Fig. 8a) exhibits almost no variation at all; the set of NOEs used is complete enough to fully define most of the molecule (Lepre et al., 1992), and there are apparently few alternative low-energy conformations simultaneously consistent with the narrow flat regions and moderately high weights of the restraints in this refinement. Note that this conformation differs significantly from the true (unrestrained) average. If this represented real data, one would erroneously conclude from the standard refinement that a single, relatively inflexible (and somewhat incorrect) conformation existed. In fact, MD-NOE refined FK506 structures in the literature derived by using narrow flat wells and high force constants have been reported as tightly defined envelopes (Karuso et al., 1990; Mierke et al., 1991). In contrast, the time-averaged refinement (Fig. 8b) yields an envelope of intermediate structures that reflect the true intrinsic flexibility quite well. In Fig. 3, the RMS atomic fluctuations about mean positions, corresponding to the simulations in Figs. 8a and 8b are compared to the 'true' unrestrained fluctuations, and quantitatively corroborate this discussion.

The ability of these restrained refinement methods to predict the true molecular behavior is related not only to the method used and the width of the flat region, but also to the force constants that are used in the restraint potential. Intuitively this can be understood by considering the limiting case where $K_u = K_l = 0$. Then the MD will not reflect the restraints and the result will be as good (or as bad!) as the force field, even if the underlying NOE distances are completely wrong.

To gauge the importance of the force constants in MD/NOE refinement, a series of simulations were carried out where the width of the flat region was fixed at a moderate value (double-sided

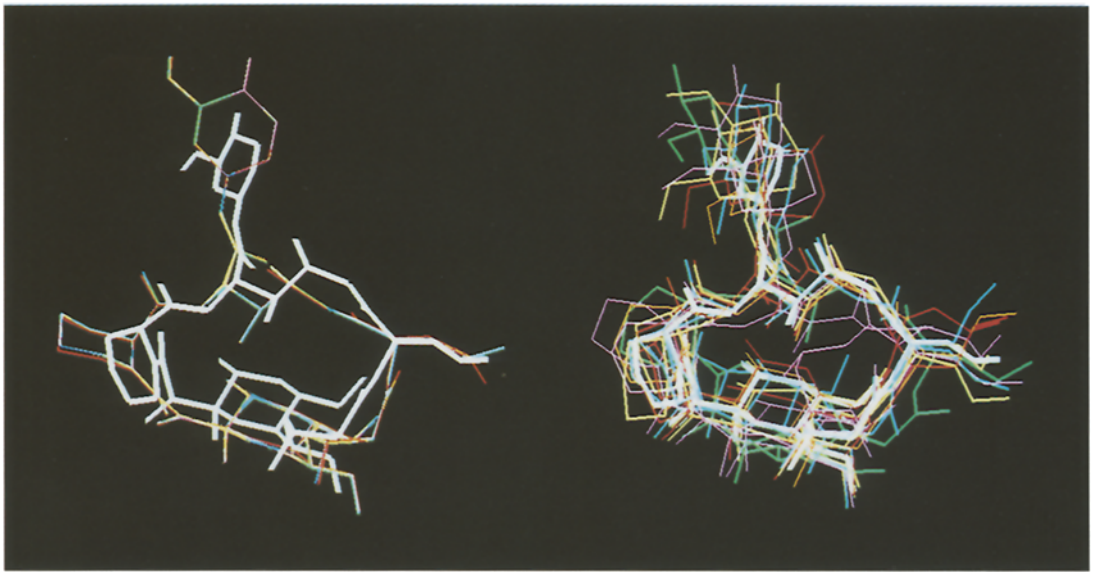

Fig. 8. Representative envelopes of conformations sampled during the refinement of FK506 using double-sided wells, $P_u = P_l = 0.75\sigma$, and $K_u = K_l = 36$ kcal/mol. An RMS best-fit superposition (using all heavy atoms) of snapshots every 100 ps along the trajectory is shown. Hydrogen atoms are not shown. The 'true' averaged conformation for the 3-ns unrestrained simulation is shown in heavy white lines. Figure 8a (left): Standard refinement; Fig. 8b (right): Time-averaged refinement.

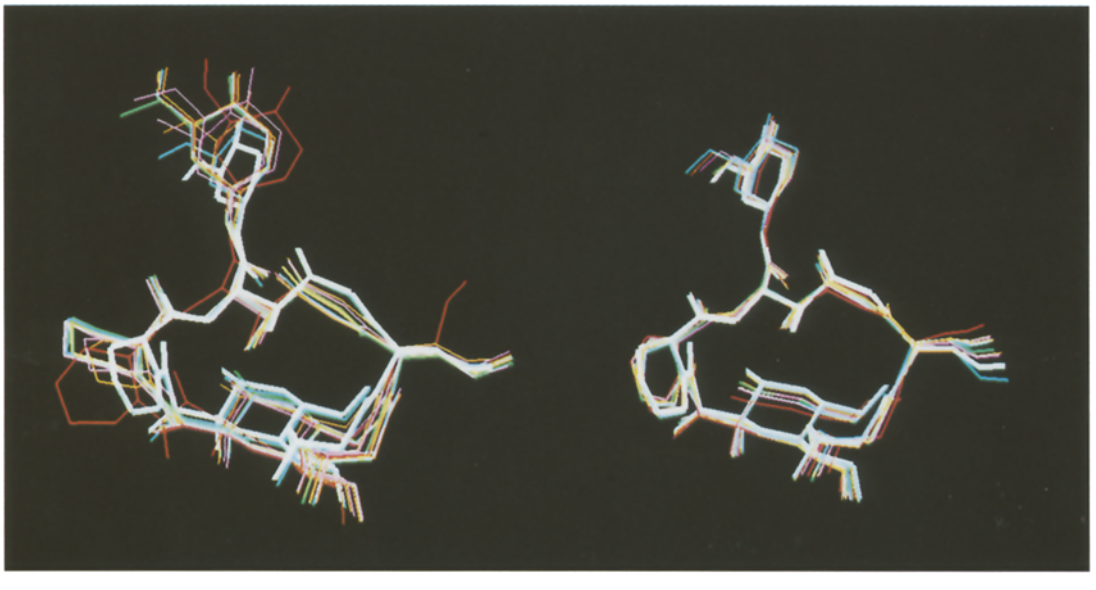

Fig. 9. The averaged conformations for the series of refinements using double-sided restraints, each with $P_u = P_l = 0.5\sigma$. The series correspond to varying values of the force constants $K_l = K_u$: 2 kcal/mol and i*4 kcal/mol, i = [1,9]. Target distances r_{NOE} were derived from the 3-ns unrestrained simulation. All averages were calculated from the final 800 ps of a 1-ns simulation. The 'true' averaged conformation for the 3-ns unrestrained simulation is shown in heavy white lines. Figure 9a (left): Standard refinement; Fig. 9b (right): Time-averaged refinement. The outlying structure in red in Fig. 9a corresponds to K = 36 kcal/mol.

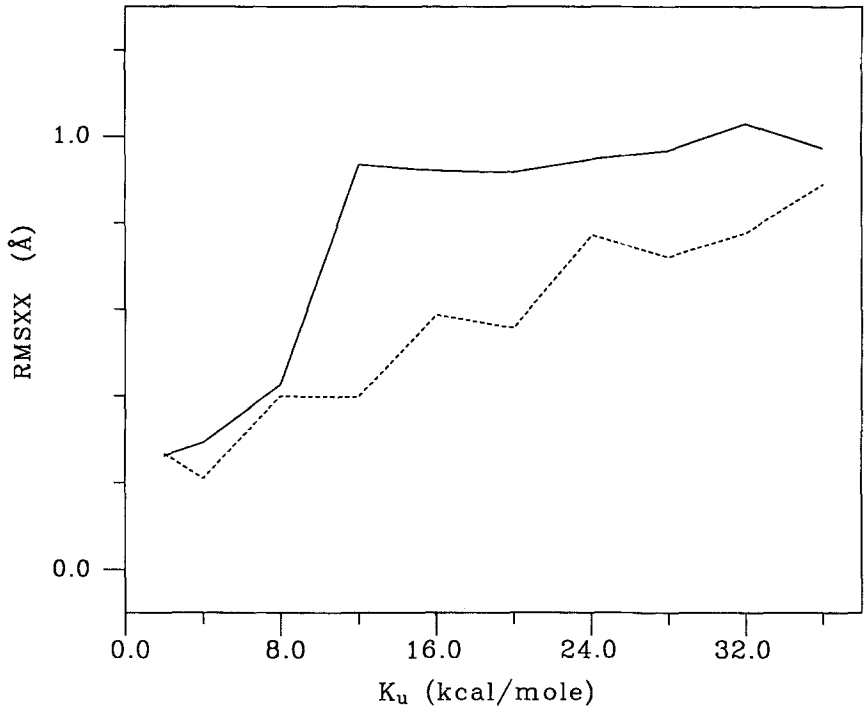

Fig. 10. RMSXX, the RMS difference between the predicted and 'true' RMS motion about mean position of all heavy atoms in the averaged structure, as a function of the force constant used. All refinements correspond to double-sided wells with $P_u = P_l = 0.5\sigma$. The refined averaged structures used to calculate the RMS differences were derived from the final 800 ps of a 1-ns simulation. The 'true' RMS motion is for the 3-ns unrestrained simulation. Solid line: Standard restraints. Dashed line: Time-averaged restraints.

wells; $P_l = P_u = 0.5\sigma$), and the force constants were varied from 2–36 kcal/mol ($K_l = K_u$). These series of simulations were run with both standard and time-averaged restraints. The averaged structures obtained are shown in Fig. 9. Once again, the averaged structures from standard restraints (Fig. 9a) display a notable sensitivity to the details of the refinement (force constants), and the result is never in complete agreement with the true average. The time-averaged simulations more accurately reproduce the average in all cases (Fig. 9b).

On the other hand, the ability of *either* method to reproduce an accurate picture of conformation flexibility *is* sensitive to the force constants used. The RMS difference between the predicted and true RMS motion of each atom in the molecule, RMSXX, is plotted as a function of force constant in Fig. 10 ($P_u = P_l = 0.5\sigma$). In this respect, simulations with small values of the force constant are considerably better. For large force constants, standard restraint simulations severely underestimate the RMS motion, while time-averaged simulations *over*estimate it (Fig. 3). The slow variation of forces in time-averaged restraints means that distance correction forces, when they occur, will be long-lasting. The result is that forces can continue after the instantaneous distances are no longer in violation. The net effect, when the forces (force constants) are inherently large, can be to exaggerate fluctuations back and forth about the equilibrium position.

As the force constants approach 0, both methods can provide a reasonable description of intrinsic flexibility (expectedly, since in the limit $K_u = K_l = 0$ they must be the same), but the

average structures from standard refinement are less reliable (Fig. 9). For larger force constants, the motion predicted by time-averaged restraints is always closer to 'reality' (the unrestrained model) than with standard restraints. Notably, even with large force constants the peaks in the time-averaged RMS plot are in the correct locations, while for standard refinement many of the regions of true flexibility are missed completely. The implied tightness of the conformational envelope for results in the literature arrived at using traditional refinement and moderate-to-large force constants is to be viewed with caution. Use of relatively large force constants in the range of 20–30 or more kcal/mol is not uncommon in the literature (Clore and Gronenborn, 1989; Gippert et al., 1990; Wagner et al., 1992).

DISCUSSION

Based on these results, we can conclude that: (1) standard refinement will tend to yield an unrealistically stiff description of conformational flexibility, and will lead to an average structure that systematically differs from the true structure and depends on the conditions (flat well width, force constants) of the refinement; and (2) time-averaged refinement provides a truer picture of conformational flexibility over a broad range of refinement conditions, and has little difficulty converging on the correct average structure, but can overestimate conformational variability when large force constants are used. While using smaller force constants gives better estimates of intrinsic motion, such force constants will frequently not be sufficient to force the initial starting guess (often from DG) to the neighborhood of the converged average conformation. We have also found that time-averaged refinement is less efficient than standard refinement at finding this neighborhood from a poor starting guess (Pearlman and Kollman, 1991). This suggests one should do an initial refinement using standard refinement, moderate force constants, and perhaps elevated temperature. Then, once a conformation in the vicinity of the average has been found, time-averaged refinement with small force constants can be run to give an appropriate average structure and a measure of its innate flexibility. Both should be reported. Keep in mind that smaller force constants increase the importance of the potential-energy force field used. One should also continue to report an energy-minimized form of the average, which can be of importance in subsequent studies such as modeling. But the intuitive simplicity of this model should not blind us to the necessity of reporting a truer picture.

The finding that the results of conventional refinement are more sensitive to the choice of flat well than those of time-averaged refinement is particularly significant. In deriving experimental NOE-based distances, sometimes only crude estimated ranges are assigned (based on the qualitative strength of the NOE signal, e.g., 'weak', 'medium' or 'strong' (Nilges et al., 1988)). Even when exact target distances are derived, flat well regions are almost always defined in recognition of experimental uncertainties. The implication of the results here is that time-averaged refinement is better able to yield a conformational envelope that reflects the true experimental behavior, regardless of the unavoidable biases introduced by inaccurate and/or qualitative distance assignments.

It is worth noting that although the time-averaged protocol offers the potential for considerable improvement in traditional NOE-derived distance refinement approaches, it is not without its own limitations. In particular, the simple reciprocal average used is only an approximation. A generally small angular dependence in the NOESY intensity–distance relationship is not taken

into account (Kessler et al., 1988). Similarly, spin diffusion effects, which will modify the apparent cross-relaxation rate between atom pairs – and hence the derived distances – are ignored during the distance refinement (Thomas et al., 1991). Fortunately, the error (flat well region) assigned to distances will frequently account for such effects, and spin diffusion effects are more likely to affect closely packed regions (regions with more nearby neighbors), where the structure will often be overdetermined. In any case, until methods which replace refinement in distance space with refinement in intensity space reach sufficient maturity to be widely applicable, we are constrained to distance-based refinement for most systems, and time averaging is an improvement on previous methods.

One thing is certain. The traditional presentation of an NMR structure as a single representative minimized structure, or as a fairly tight envelope of conformers meeting imposed distance restraints in standard refinement, can be misleading. Our ideas of what constitutes an experimental 'structure' and of how we arrive at that structure need to be revised to better reflect reality and not model simplicities. The concepts of time-averaging discussed here can also be applied to crystallography (Gros et al., 1990) and a movement towards greater acknowledgement of the inherent flexibility of molecules is equally important in that field.

ACKNOWLEDGEMENTS

We are grateful to Drs. Chris Lepre and Jon Moore for numerous helpful suggestions and for providing a preprint of their solution structure determination of FK506. We also thank Drs. Mark Murcko and Jya-Wei Cheng for critical reading of the manuscript, Sergio Rotstein for help taking the pictures and Greg Moody, Ron Johnson and Brian Perry for maintenance and administration of the computers on which this work was performed.

REFERENCES

Baleja, J.D., Germann, M.W., van de Sande, J.H. and Sykes, B.D. (1990) *J. Mol. Biol.*, **215**, 411–428.
Blundell, T. and Johnson, L.N. (1976) *Protein Crystallography*, Academic Press, New York, NY.
Bonvin, A.M.J.J., Boelens, R. and Kaptein, R. (1991) *J. Magn. Reson.*, **95**, 626–631.
Borgias, B.A. and James, T.L. (1988) *J. Magn. Reson.*, **79**, 493–512.
Brunger, A.T. and Karplus, M. (1991) *Acc. Chem. Res.*, **24**, 54–61.
Burkert, U. and Allinger, N.L. (1982) *Molecular Mechanics, ACS Monographs*, Vol. 177, American Chemical Society, Washington, DC.
Clark, T. (1985) *A Handbook of Computational Chemistry*, Wiley, New York, NY.
Clore, G.M. and Gronenborn, A.M. (1989) *Crit. Rev. Biochem. Mol. Biol.*, **24**, 479–564.
Crippen, G.M. and Havel, T.F. (1988) *Distance Geometry and Molecular Conformation*, Wiley, New York, NY.
Dellwo, M.J. and Wand, A.J. (1989) *J. Am. Chem. Soc.*, **111**, 4571–4578.
Edmondson, S.P. (1992) *J. Magn. Reson.*, **98**, 283–298.
Elber, R. and Karplus, M. (1987) *Science*, **235**, 318–321.
Gippert, G.P., Yip, P.F., Wright, P.E. and Case, D.A. (1990) *Biochem. Pharmacol.*, **40**, 15–22.
Gros, P., van Gunsteren, W.F. and Hol, W.G.J. (1990) *Science*, **249**, 1149–1152.
Havel, T.F. (1991) *Prog. Biophys. Mol. Biol.*, **56**, 43–78.
James, T.L. and Basus, V.J. (1991) *Annu. Rev. Phys. Chem.*, **42**, 501–542.
Kaptein, R., Boelens, R., Scheek, R.M. and van Gunsteren, W.F. (1988) *Biochemistry*, **27**, 5389–5395.
Karuso, P., Kessler, H. and Mierke, D.F. (1990) *J. Am. Chem. Soc.*, **112**, 9434–9436.
Kessler, H., Griesinger, C., Lautz, J., Muller, A., van Gunsteren, W.F. and Berendsen, H.J.C. (1988) *J. Am. Chem. Soc.*, **110**, 3393–3396.

Lane, A.N. (1990) *Biochim. Biophys. Acta,* **1049**, 189–204.
Lepre, C.A., Thomson, J.A. and Moore, J.M. (1992) *FEBS Lett.*, **302**, 89–96.
Liu, Y., Zhao, D., Altman, R. and Jardetsky, O. (1992) *J. Biomol. NMR*, **2**, 373–388.
Mierke, D.F., Schmieder, P., Karuso, P. and Kessler, H. (1991) *Helv. Chim. Acta*, **74**, 1027–1047.
Mirau, P.A. (1992) *J. Magn. Reson.*, **96**, 480–490.
Nerdal, W., Hare, D.R. and Reid, B.R. (1989) *Biochemistry*, **28**, 10008–10021.
Nilges, M., Clore, G.M. and Gronenborn, A.M. (1988) *FEBS Lett.*, **229**, 317–324.
Nilges, M., Habazettl, J., Brunger, A.T. and Holak, T.A. (1991) *J. Mol. Biol.*, **219**, 499–510.
Pearlman, D.A., Case, D.A., Caldwell, J.C., Seibel, G.L., Singh, U.C., Weiner, P. and Kollman, P.A. (1991) *AMBER 4.0*, University of California, San Francisco, CA.
Pearlman, D.A. and Kollman, P.A. (1991) *J. Mol. Biol.*, **220**, 457–479.
Petsko, G. and Ringe, D. (1984) *Annu. Rev. Biophys.*, **13**, 331–371.
Pranata, J. and Jorgensen, W.L. (1991) *J. Am. Chem. Soc.*, **113**, 9483–9493.
Schreiber, S.L. (1991) *Science*, **251**, 283–287.
Smith, J.C. (1991) *Q. Rev. Biophys.*, **24**, 227–291.
Thomas, P.D., Basus, V.J. and James, T.L. (1991) *Proc. Natl. Acad. Sci. USA*, **88**, 1237–1241.
Torda, A.E., Scheek, R.M. and van Gunsteren, W.F. (1989) *Chem. Phys. Lett.*, **157**, 289–294.
Torda, A.E., Scheek, R.M. and van Gunsteren, W.F. (1990) *J. Mol. Biol.*, **214**, 223–235.
Van Duyne, G.D., Standaert, R.F., Karplus, P.A., Schreiber, S.L. and Clardy, J. (1991) *Science*, **252**, 839–842.
Wagner, G., Hyberts, S.G. and Havel, T.F. (1992) *Annu. Rev. Biophys. Biomol. Struct.*, **21**, 167–198.
Wagner, G. and Wüthrich, K. (1979) *J. Magn. Reson.*, **33**, 675–680.
Weiner, S.J., Kollmann, P.A., Nguyen, D.T. and Case, D.A. (1986) *J. Comput. Chem.*, **7**, 230–252.
Wüthrich, K. (1986) *NMR of Proteins and Nucleic Acids*, Wiley, New York, NY.
Wüthrich, K. (1990) *J. Biol. Chem.*, **265**, 22059–22062.
Yip, P. and Case, D.A. (1989) *J. Magn. Reson.*, **83**, 643–648.